Deletion of tumor necrosis factor death receptor inhibits amyloid β generation and prevents learning and memory deficits in Alzheimer's mice

Ping He,[1] Zhenyu Zhong,[1] Kristina Lindholm,[1] Lilian Berning,[1] Wendy Lee,[1] Cynthia Lemere,[3] Matthias Staufenbiel,[4] Rena Li,[2] and Yong Shen[1]

[1]Haldeman Laboratory of Molecular and Cellular Neurobiology and [2]Roberts Center for Alzheimer's Research, Sun Health Research Institute, Sun City, AZ 85351
[3]Center for Neurologic Diseases, Brigham and Women's Hospital, Harvard Medical School, Boston, MA 02115
[4]Novartis Pharma Ltd., Nervous System Research, CH-4002 Basel, Switzerland

The tumor necrosis factor type 1 death receptor (TNFR1) contributes to apoptosis. TNFR1, a subgroup of the TNFR superfamily, contains a cytoplasmic death domain. We recently demonstrated that the TNFR1 cascade is required for amyloid β protein (Aβ)–induced neuronal death. However, the function of TNFR1 in Aβ plaque pathology and amyloid precursor protein (APP) processing in Alzheimer's disease (AD) remains unclear. We report that the deletion of the TNFR1 gene in APP23 transgenic mice (APP23/TNFR1$^{-/-}$) inhibits Aβ generation and diminishes Aβ plaque formation in the brain. Genetic deletion of TNFR1 leads to reduced β-secretase 1 (BACE1) levels and activity. TNFR1 regulates BACE1 promoter activity via the nuclear factor-κB pathway, and the deletion of TNFR1 in APP23 transgenic mice prevents learning and memory deficits. These findings suggest that TNFR1 not only contributes to neurodegeneration but also that it is involved in APP processing and Aβ plaque formation. Thus, TNFR1 is a novel therapeutic target for AD.

Introduction

Alzheimer's disease (AD) affects ∼4.5 million Americans, and this number will continue to grow. By 2050, the number of individuals with AD could range from 11.3 to 16 million (Hebert et al., 2003). The pathogenesis underlying AD remains unclear, and it is controversial whether AD results from a primary abnormality in amyloid precursor protein (APP) or deregulation of the inflammatory system (Weiner and Selkoe, 2002), although these two possibilities are not mutually exclusive. Several lines of evidence implicate abnormal processing of APP, which is cleaved by two enzymes, β-secretase 1 (BACE1) and γ-secretase, to generate excessive amyloid β protein (Aβ), as a potential cause of AD (Selkoe, 2003; Tanzi and Bertram, 2005). In the past decade, transgenic mice have been generated that overexpress mutant APP and display Aβ-related lesions (Hsiao et al., 1995). Many of these mouse models exhibit amyloid plaque-predominant aspects of AD (Terry et al., 1987; Tiraboschi et al., 2004), including Aβ plaque formation, cerebral amyloid angiopathy (CAA), and inflammation, but not τ pathology.

The TNF death receptor belongs to the *TNFR* superfamily, which includes >20 cell surface receptors. When the TNF type 1 death receptor (TNFR1) binds to its ligand, TNFα, the ligand–receptor complex triggers apoptotic pathways by recruiting a TNFR-associated death domain protein and/or a Fas-associated death domain protein/mediator of receptor-induced toxicity, two intracellular adaptor proteins (Boldin et al., 1995). The receptor-induced multimerization of a Fas-associated death domain protein leads to caspase activation, which causes degradation of specific target proteins, ultimately damaging cell integrity (Ashkenazi and Dixit, 1998).

To find out whether TNFR1 could have effect on Aβ production as well as APP processing, we specifically chose transgenic APP23 mice in our experiments, which express a mutant APP that results in extensive Aβ plaque formation. Here we show that fewer Aβ plaques and Aβ-related lesions develop in Alzheimer's transgenic mice with genetic deletion of *TNFR1*. Detailed analyses showed decreased Aβ generation, less neuronal loss, and alleviated Aβ-related memory deficits. Our data indicates that *TNFR1* might be a potential and novel therapeutic target for AD.

P. He and Z. Zhong contributed equally to this paper.

Correspondence to Yong Shen: yong.shen@sunhealth.org

Abbreviations used in this paper: Aβ, amyloid β protein; AD, Alzheimer's disease; ANOVA, analysis of variance; APP, amyloid precursor protein; BACE1, β-secretase 1; CAA, cerebral amyloid angiopathy; IDE, insulin degradation enzyme; NEP, neprilysin; NF-κB, nuclear factor κB; TNFR1, TNF type 1 death receptor; vWF, von Willebrand factor.

The Journal of Cell Biology, Vol. 178, No. 5, August 27, 2007 829–841
http://www.jcb.org/cgi/doi/10.1083/jcb.200705042

Results

TNFR1 deletion reduces Aβ-related pathology

APP23 transgenic mice (Sommer and Staufenbiel, 1998), a mouse model for AD with a plaque-predominant type (Terry et al., 1987; Tiraboschi et al., 2004), overproduce Aβ, Aβ40, and Aβ42, and develop significant amyloid deposits by the age of 14 mo. To determine whether genetic inactivation of *TNFR1* delays or diminishes Aβ plaque formation, we crossed APP23 mice with mice lacking the *TNFR1* gene (*TNFR1*$^{-/-}$; Peschon et al., 1998) to generate APP23/*TNFR1*$^{-/-}$ mice. To evaluate Aβ pathology in the brains, we first used Congo red staining to see if reduced protein aggregation could be observed in the brains of APP23/*TNFR1*$^{-/-}$ mice. Congo red has been shown to be affinitive for binding to fibril proteins enriched in β-sheet conformation, and it is commonly used as a histological dye for amyloid detection (Frid et al., 2006). Results showed much less Congo red staining in APP23/*TNFR1*$^{-/-}$ mice (Fig. 1 A), indicating that protein aggregation was alleviated in APP23/*TNFR1*$^{-/-}$ mice.

To further confirm that the aggregated protein we found was aggregated Aβ peptide, we next examined the brain section with anti-Aβ antibody 6E10 (Vassar et al., 1999; Van Dooren et al. 2006). At 12 mo of age, APP23 mice displayed numerous Aβ plaques throughout the entorhinal cortex and hippocampus, consistent with a previous paper (Sommer and Staufenbiel, 1998). In APP23/*TNFR1*$^{-/-}$ mice, however, we found only minor Aβ plaques in the entorhinal cortex (Fig. 1, B and C) and the hippocampus (Fig. 1, D and E). At 24 mo of age, APP23/*TNFR1*$^{-/-}$ mice also displayed reduced plaques (Fig. 1, B and D). The number of plaques was reduced by 73 and 80% in the entorhinal cortex (Fig. 1 C) and hippocampus (Fig. 1 E) in APP23/*TNFR1*$^{-/-}$ mice at 12 mo of age, indicating that Aβ pathology in APP23/*TNFR1*$^{-/-}$ indeed alleviated plaque formation compared with age-matched APP23 mice.

The size of Aβ plaques also indicates the severity of Aβ pathology (Zhou et al., 2005). We used morphometric analyses on the brain sections immunostained with Aβ antibody 6E10. Results showed that both large (>20 μm diameter)- and medium (10–20 μm diameter)-sized Aβ plaques in the entorhinal cortex (Fig. 1 F) and hippocampus (Fig. 1 G) were significantly reduced in APP23/*TNFR1*$^{-/-}$ mice at 12 and 24 mo of age, indicating that in APP23/*TNFR1*$^{-/-}$ mice, Aβ pathology was alleviated not only by reducing the overall Aβ plaque number, but also by decreasing plaque size.

TNFR1 deletion reduces CAA

CAA has been reported to have both positive and negative correlations with AD pathology (Cohen et al., 1997; Thal et al., 2003; Tian et al., 2003). It has been shown that CAA in APP23 transgenic mice is strikingly similar to that of human CAA (Calhoun et al., 1999). To find out whether genetic deletion of *TNFR1* can relieve CAA in APP23 mice, the deposition of Aβ in the vascular wall was examined by double immunostaining with antibodies against β-smooth muscle actin (a vascular smooth muscle marker; Skalli et al., 1986) or von Willebrand factor (vWF; an endothelial cell marker; Shyu et al., 2006) and anti-Aβ40 antibody. We found that at 24 mo of age, APP23 mice display CAA predominant in cortical, hippocampal, and thalamic vessels; Aβ40 formed a continuous ring-like shape within the vessel wall (Fig. 2, A and B), consistent with Calhoun et al. (1999). However, there were very few Aβ40 deposits within the vessels of APP23/*TNFR1*$^{-/-}$ (Fig. 2, C and D). Deposition of Aβ on the vascular wall could not only increase the vulnerability of cerebral vessels but also increase the possibility of intracerebral hemorrhage (Vinters, 1987; Itoh et al., 1993; Winkler et al., 2001; Atwood et al., 2003). Our results showed little CAA progression in the brains of APP23/*TNFR1*$^{-/-}$ mice, suggesting that deletion of *TNFR1* could reduce the risk of CAA.

TNFR1 deletion reduces microglia activation

Microglia activation is also a hallmark of Aβ pathology progression (Yan et al., 2003 ;Wilcock et al., 2004; Simard et al., 2006). CD11b and CD45 are two well-characterized markers for microglia activation in the brains (Yan et al., 2003; Wilcock et al., 2004; Simard et al., 2006).To examine whether deletion of *TNFR1* could alleviate the massive microglia activation of APP23 mice, we studied the microglia activation in APP23 and APP23/*TNFR1*$^{-/-}$ mice. Consistent with a previous paper (Wilcock et al., 2003), APP23 mice showed strong immunoreactivity with antibodies against CD11b (Mac-1) and CD45 in the entorhinal cortex (Fig. 3 A) and hippocampus (Fig. 3 B), indicating that a massive amount of microglia had been activated along with the appearance of Aβ pathology. In contrast, APP23/*TNFR1*$^{-/-}$ mice showed significantly less CD11b and CD45 immunoreactivity in the entorhinal cortex (Fig. 3 A) and hippocampus (Fig. 3 B), indicating that genetic deletion of *TNFR1* alleviated massive microglia activation in APP23 mice.

TNFR1 deletion reduces Aβ production

Because we found reduced Aβ pathology in APP23/*TNFR1*$^{-/-}$ mice, our next question was whether genetic inactivation of *TNFR1* reduces Aβ pathology by affecting Aβ generation. The Aβ level was analyzed by immunoprecipitation followed by Western blotting ($n = 3$ for each group). Fig. 4 A shows a representative urea Western blot (Wiltfang et al., 1997) comparing the 4-kD Aβ species ($n = 3$ for each group). Both Aβ40 and Aβ42 can be detected, and Aβ42 migrated ahead of Aβ40, consistent with a previous paper (Wiltfang et al., 1997). Compared with APP23 mice, APP23/*TNFR1*$^{-/-}$ mice showed a significant reduction in both Aβ40 and Aβ42 levels (Fig. 4 A). We further measured total Aβ, Aβ40, and Aβ42 levels by sandwich ELISAs ($n = 10$ for each group). The results bolstered our Western blot findings and confirmed that APP23/*TNFR1*$^{-/-}$ mice have much less total Aβ, Aβ40, and Aβ42 (Fig. 4, B–D). Quantitatively, total Aβ decreased by 69% (37.39 ± 12.71 ng/mg) and 30% (463.87 ± 189.83 ng/mg) in 12- and 24-mo-old APP23/*TNFR1*$^{-/-}$ mice, respectively, compared with total Aβ in APP23 mice (12 mo old: 120.80 ± 39.74 ng/mg; 24 mo old: 693.40 ± 270.27 ng/mg; Fig. 4 B). Both Aβ40 and Aβ42 were reduced in APP23/*TNFR1*$^{-/-}$ mice. However, the most significant difference is at 12 mo of age, when Aβ40 decreased by 80% in

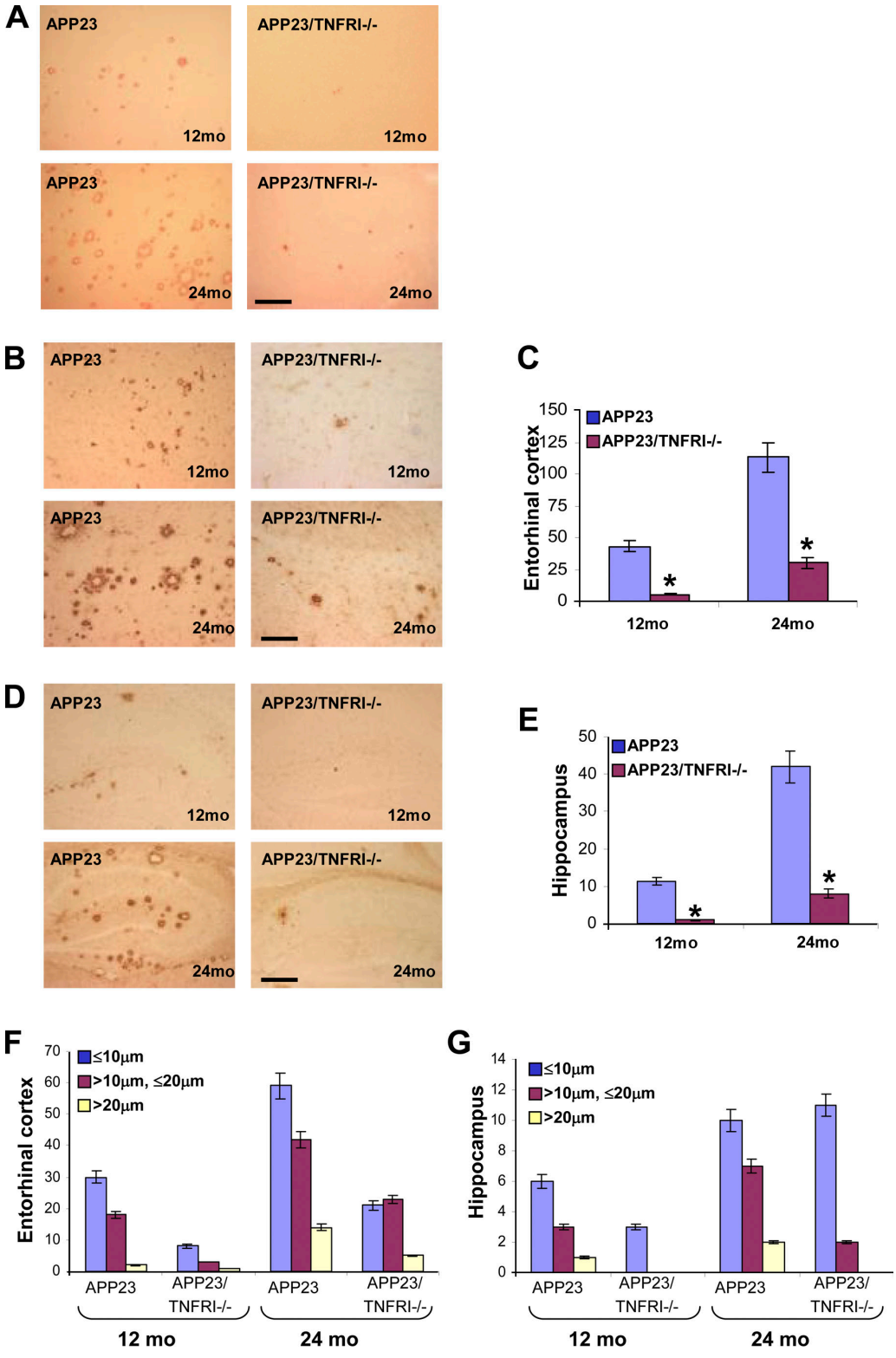

Figure 1. **Aβ deposition is significantly reduced in APP23/*TNFR1*$^{-/-}$ mice.** (A) Congo red showed fewer congophilic deposits in the brains of APP23/*TNFR1*$^{-/-}$ mice at both 12 and 24 mo of age. (B) 6E10-immunostained sections of the entorhinal cortex. (C) Stereological analyses of 6E10-immunostained sections revealed fewer immunoreactive plaques in the entorhinal cortex of APP23/*TNFR1*$^{-/-}$ mice. (D) 6E10-immunostained sections of the hippocampus. (E) Stereological analyses of 6E10-immunostained sections revealed fewer immunoreactive plaques in the hippocampus of APP23/*TNFR1*$^{-/-}$ mice (*, $P < 0.05$). (F) Fewer large plaques (>20 μm) were found in the entorhinal cortex of APP23/*TNFR1*$^{-/-}$ mice. (G) Fewer large plaques (>20 μm) were found in the hippocampus of APP23/*TNFR1*$^{-/-}$ mice. Error bars represent SD. Bars, 50 μm.

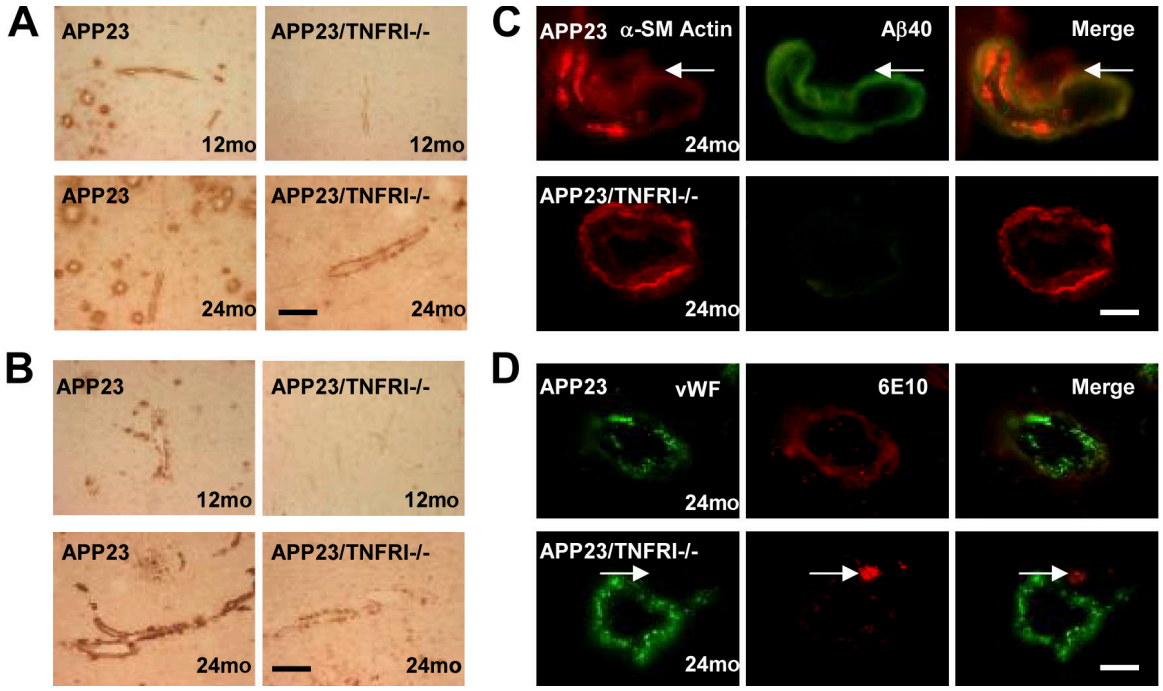

Figure 2. **Cerebral vascular amyloid deposits were reduced in APP23/*TNFR1*$^{-/-}$ mice.** (A) 6E10 immunostaining showed that microvascular Aβ deposits were reduced in the frontal cortex of APP23/*TNFR1*$^{-/-}$ mice. (B) Vascular Aβ deposits were reduced in the thalamus of APP23/*TNFR1*$^{-/-}$ mice. (C) Double labeling of α-smooth muscle actin (α-SM actin; red) and Aβ40 (green) showed fewer Aβ40 deposits on microvascular walls of 24-mo-old APP23/*TNFR1*$^{-/-}$ mice than in age-matched APP23 mice (arrow points to absence of Aβ deposits on one smaller vascular wall). (D) Double labeling of 6E10 and vWF antibody showed fewer Aβ deposits on the vascular walls of 24-mo-old APP23/*TNFR1*$^{-/-}$ mice (arrow points to an Aβ plaque that appears to be outside of the vascular wall in the cortex of APP23/*TNFR1*$^{-/-}$ mice). Bars: (A and B) 50 μm; (C and D) 5 μm.

APP23/*TNFR1*$^{-/-}$ mice (20.45 ± 4.7 ng/mg) compared with APP23 mice (103.87 ± 21.81 ng/mg; Fig. 4 C), and Aβ42-decreased by 70% in APP23/*TNFR1*$^{-/-}$ mice (4.12 ± 1.2 ng/mg) compared to APP23 mice (15.78 ± 4.7 ng/mg; Fig. 4 D). These results indicated that reduction in Aβ40 and Aβ42 levels could account for the alleviated Aβ pathology in APP23/*TNFR1*$^{-/-}$ mice.

One of the mechanisms that could influence Aβ production is through altering APP holoprotein levels. We next analyzed by Western blot to see if deletion of *TNFR1* affects APP protein levels ($n = 3$ for each group). In contrast to the reduction in Aβ levels, Western blotting did not reveal any differences in full-length APP levels between APP23/*TNFR1*$^{-/-}$ and APP23 mice (Fig. 4 E), indicating that the decrease in Aβ levels was not caused by altering APP protein expression in APP23/*TNFR1*$^{-/-}$ mice.

TNFR1 deletion alters BACE1 activity and level

To examine whether the reduced amyloidosis in APP23/*TNFR1*$^{-/-}$ mice was caused by a reduction in abnormal APP metabolism, we examined the activity and expression levels of one key enzyme in APP processing, BACE1.

We first used an MCA-labeled BACE1 substrate (Yang et al., 2003; Li et al., 2004a) to examine BACE1 activity and found that BACE1 activity was significantly decreased in APP23/*TNFR1*$^{-/-}$ mice (Fig. 5 A). To find out whether the decreased BACE1 activity was due to a decrease in BACE1 levels, we measured BACE1 levels by sandwich ELISA (Yang et al., 2003) and Western blot ($n = 3$ for each group). We found that BACE1 levels in APP23/*TNFR1*$^{-/-}$ mice were indeed reduced in both Western blot and ELISA results (Fig. 5, B and C), indicating that reduced BACE1 activity in APP23/*TNFR1*$^{-/-}$ mice was caused by a reduction in the protein level. To further investigate whether reduced BACE1 protein level is caused by reduced BACE1 mRNA transcription, we performed RT-PCR to measure BACE1 mRNA levels and found that BACE1 mRNA was also decreased in APP23/*TNFR1*$^{-/-}$ mice (Fig. 5 D), indicating that the genetic deletion of *TNFR1* reduced BACE1 mRNA levels and caused BACE1 activity to be down-regulated in APP23/*TNFR1*$^{-/-}$ mice.

TNFα regulates BACE1 transcription through the TNFR1–nuclear factor κB (NF-κB) pathway

Our RT-PCR results showed that BACE1 mRNA levels decreased in APP23/*TNFR1*$^{-/-}$ mice; the next question was what signal transduction pathway leads to the decreased BACE1 mRNA level.

To clarify how deletion of *TNFR1* affects BACE1, we transfected 293 cells with a pB1P-A vector containing a *BACE1* promoter (−1941 to +292) that was upstream of a luciferase reporter gene (Christensen et al., 2004; Sambamurti et al., 2004), and then treated these cells with different concentrations of TNFα. We found that BACE1 promoter activity increased in a concentration-dependent manner (Fig. 6 A). Blocking the interaction of TNFα with the extracellular domain fragment of TNFR1 inhibited such elevation in BACE1 promoter activity (Fig. 6 A), indicating that TNFα activates BACE1 promoter through *TNFR1*.

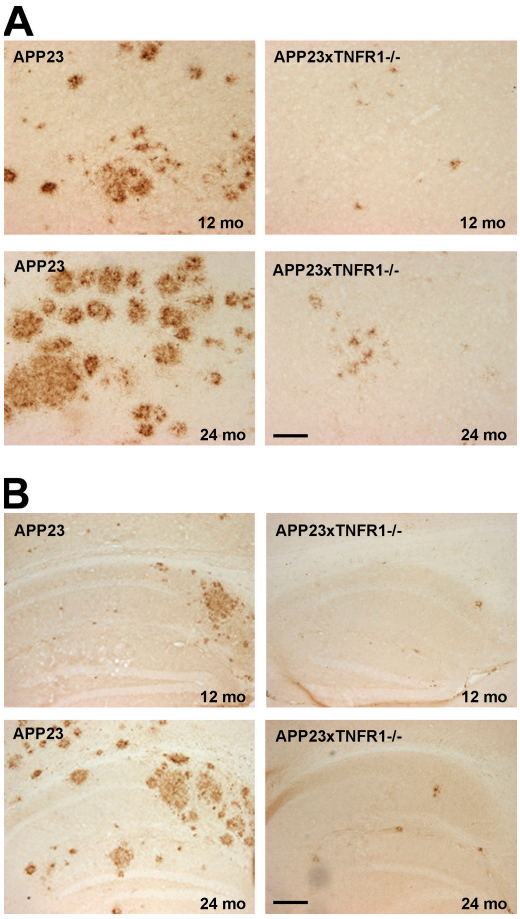

Figure 3. **Microglia activation is reduced in the brains of APP23/*TNFR1*$^{-/-}$ mice.** (A) The sections were immunostained with CD11b, an activated microglia marker, in the entorhinal cortex. (B) The sections were immunostained with CD11b in the hippocampus. Bars, 50 μm.

NF-κB is one of the major mediators of TNFα-activated *TNFR1* signaling (Hsu et al., 1995; Yang et al., 2002). A recent finding that multiple NF-κB binding sites are located in the vicinity of BACE1 promoter (Sambamurti et al., 2004) suggests that NF-κB may play an important role in regulating BACE1 transcription. To determine whether *TNFR1* activates the BACE1 promoter through this pathway, we used the potent NF-κB activation inhibitor 6-amino-4(4-phenoxyphenylethylamino) quinazoline (Tobe et al., 2003) to block NF-κB signaling in TNFα-treated 293 cells transfected with a BACE1 promoter luciferase reporter vector. Treating a pB1P-A transfected cell with an NF-κB inhibitor significantly reduced TNFα-induced BACE1 promoter activity (Fig. 6 B). A high concentration of NF-κB inhibitor inhibited not only TNFα-induced BACE1 promoter activity but also basal promoter activity (Fig. 6 B), indicating that NF-κB may play a central role in regulating BACE1 transcription. Thus, the TNFα-mediated activation of NF-κB through *TNFR1* represents a key part of this regulatory pathway.

These findings indicate that one mechanism underlying the regulation of BACE1 transcription may be through *TNFR1*-mediated activation of NF-κB. We found significantly lower Aβ as well as BACE1 levels in APP23/*TNFR1*$^{-/-}$ in older specimens (12 and 24 mo). One possible explanation is that when Aβ deposits are lower (at both time points), there is less Aβ to extract, therefore lower Aβ levels might not be caused by the reduced BACE1 level. To examine whether the reduced Aβ level is caused by the reduced BACE1 level, we measured Aβ and BACE1 levels in APP23/*TNFR1*$^{-/-}$ mice at 6 mo of age, before Aβ pathology can be observed. If *TNFR1* affects the BACE1 level, it should also reduce the BACE1 level at this age. We first found that total Aβ in APP23/*TNFR1*$^{-/-}$ mice was much lower than in APP23 mice (Fig. 7 A). Both Aβ40 and Aβ42 levels in APP23/*TNFR1*$^{-/-}$ mice were also reduced. A Western blot showed a reduction of the BACE1 protein level in APP23/*TNFR1*$^{-/-}$ mice (Fig. 7 B). BACE1 RT-PCR showed a similar result to that of 12-mo-old mice; the BACE1 mRNA level was significantly lower in APP23/*TNFR1*$^{-/-}$ mice than in APP23 mice (Fig. 7 C). Together, these findings indicate that *TNFR1* indeed regulates the BACE1 mRNA level, and that Aβ reduction in APP23 mice after genetic deletion of *TNFR1* is caused by decreased BACE1 levels.

TNFR1 deletion has little effect on Aβ clearance enzymes insulin degradation enzyme (IDE) and neprilysin (NEP)

Aβ reduction could also be caused by an increase in Aβ degradation/clearance activity, which is not relevant to Aβ production. To determine whether deletion of *TNFR1* reduces Aβ deposition by affecting enzymes involved in Aβ degradation, we assessed the protein levels of IDE and NEP, two enzymes that play an important role in Aβ degradation and clearance (Farris et al., 2003). Western blot analyses did not show significant differences in either IDE or NEP levels between APP23/*TNFR1*$^{-/-}$ and APP23 mice (Fig. 8 A), suggesting that deletion of *TNFR1* did not interfere with IDE and NEP expression. To find out whether deletion of *TNFR1* could have an effect on IDE or NEP activity, we further compared both IDE and NEP activity between APP23 and APP23/*TNFR1*$^{-/-}$ mice. Again, no significant difference was observed (Fig. 8, B and C). Therefore, IDE and NEP were not responsible for the reduction of the Aβ level associated with the *TNFR1* deletion.

TNFR1 deletion ameliorates neuron loss

We recently reported that *TNFR1* plays a critical role in Aβ-induced neuronal death (Li et al., 2004b). To determine whether the deletion of *TNFR1* protects neurons, we compared neuronal loss in wild-type, APP23/*TNFR1*$^{-/-}$, and APP23 mice. Compared with wild-type mice, APP23 mice show a 30% reduction in NeuN-positive cells in the entorhinal cortex, whereas APP23/*TNFR1*$^{-/-}$ mice show no significant reduction at 24 mo of age (Fig. 9, A and C). Results were similar in the hippocampus, where APP23 mice had 15% fewer NeuN-positive cells in the CA1 area of the hippocampus (Fig. 9 B, D; Calhoun et al., 1998), whereas little neuronal loss was seen in APP23/*TNFR1*$^{-/-}$ mice at 24 mo of age (Fig. 9, B and D). We found similar results using Nissl-stained brain sections (not depicted).

TNFR1 deletion lessens memory deficits typical of APP23 mice

To examine the behavioral significance of *TNFR1* deletion, we tested wild-type, APP23, APP23/*TNFR1*$^{-/-}$, and *TNFR1*$^{-/-}$

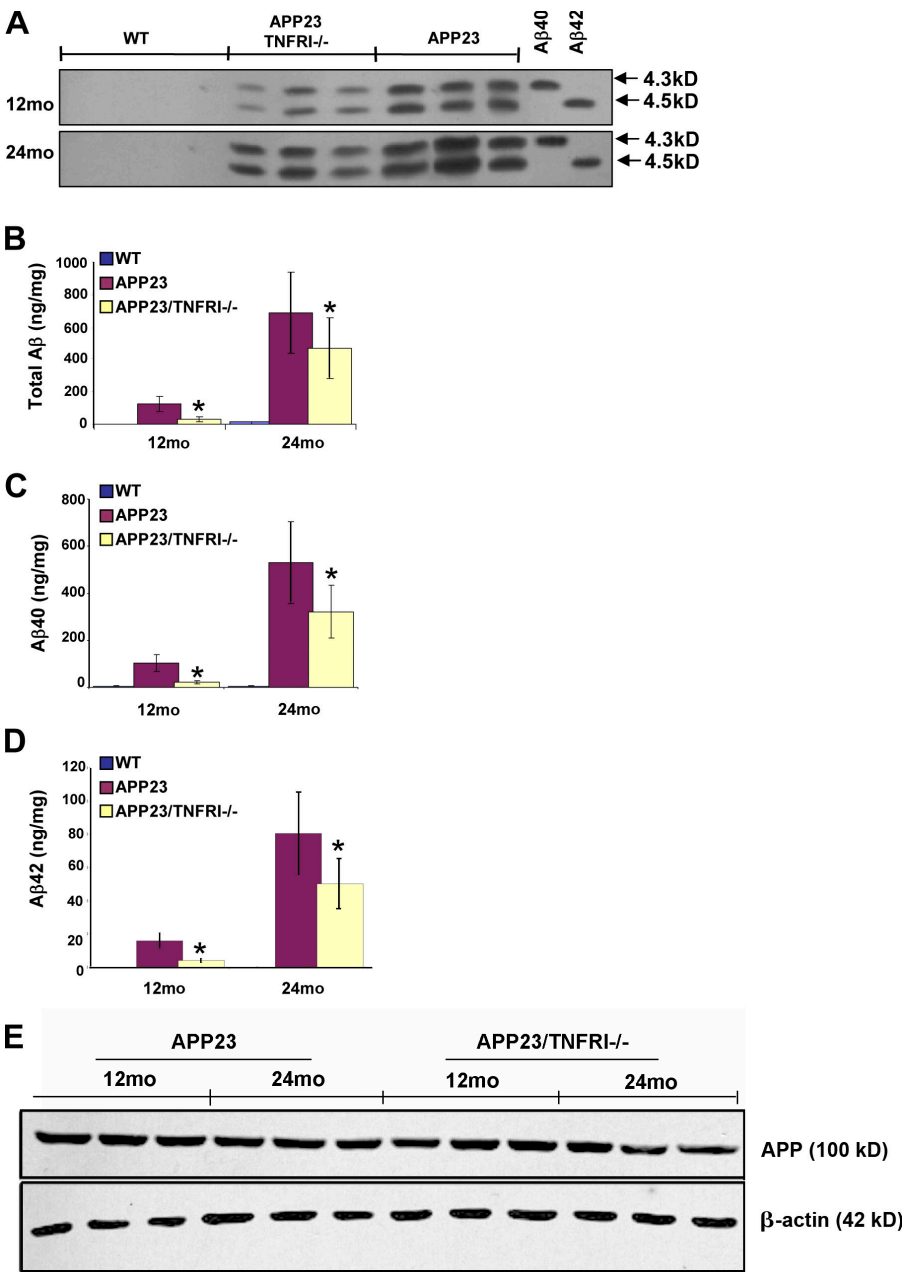

Figure 4. **Deletion of *TNFR1* reduces Aβ production.** (A) Western blot showed reduced Aβ40 and Aβ42 in APP23/*TNFR1*$^{-/-}$ mice at both 12 and 24 mo of age. (B) Total Aβ ELISA was calculated as nanogram per milligram of protein. (C) Aβ40 ELISA was calculated as nanogram per milligram of protein. (D) Aβ42 ELISA was calculated as picogram per milligram of protein (*, $P < 0.05$). (E) Western blot of brain lysates (50 μg protein) showed the APP expression. No change in APP expression was observed. Error bars represent SD.

mice with a hole-board memory test, which is a behavioral task widely used to assess exploratory learning and memory (Garcia, 1987; Thifault et al., 2002). The majority of APP23 mice showed significant deficits in the spatial component of the test. However, exploratory learning and memory retention (percentage of correct pokes) of APP23/*TNFR1*$^{-/-}$ mice was not significantly different from that of wild-type or *TNFR1*$^{-/-}$ mice (Fig. 10 A). This suggests that deletion of *TNFR1*, which could lead to a reduction of Aβ levels as well as neuronal protection, might have an effect on improving spatial learning performance in APP23/*TNFR1*$^{-/-}$ mice (Fig. 10 A). The correlation between Aβ reduction/neuronal protection and improved learning and memory behaviors remained strong when the percentages of correct pokes were averaged over all hidden hole-board trials (Fig. 10 A). Specifically, we found that 6-mo-old APP23 mice made more errors than did age-matched wild-type mice across 3 d of testing (group effect, $F1,15 = 22.198$, $P < 0.001$). However, percentage correct scores of APP23/*TNFR1*$^{-/-}$ mice were markedly higher than those of APP23 mice. APP23/*TNFR1*$^{-/-}$ mice made significantly fewer errors than did APP23 mice on days 2 and 3 of testing (group effect, $F1,20 = 8.957$, $P < 0.05$).

The object recognition task is based on the spontaneous exploration of novel and familiar objects. Mice will spend more time exploring a novel object than a familiar one (Pittenger et al., 2002; Bourtchouladze et al., 2003; Wang et al., 2004). We further examined whether deletion of *TNFR1* could rescue object recognition deficits in APP23 mice. Object recognition performance was much better in APP23/*TNFR1*$^{-/-}$ mice than in APP23 mice, as the recognition indexes differed significantly between these groups (group effect, $F3,31 = 24.947$, $P < 0.001$; Fig. 10 B). APP23/*TNFR1*$^{-/-}$ mice performed comparably to

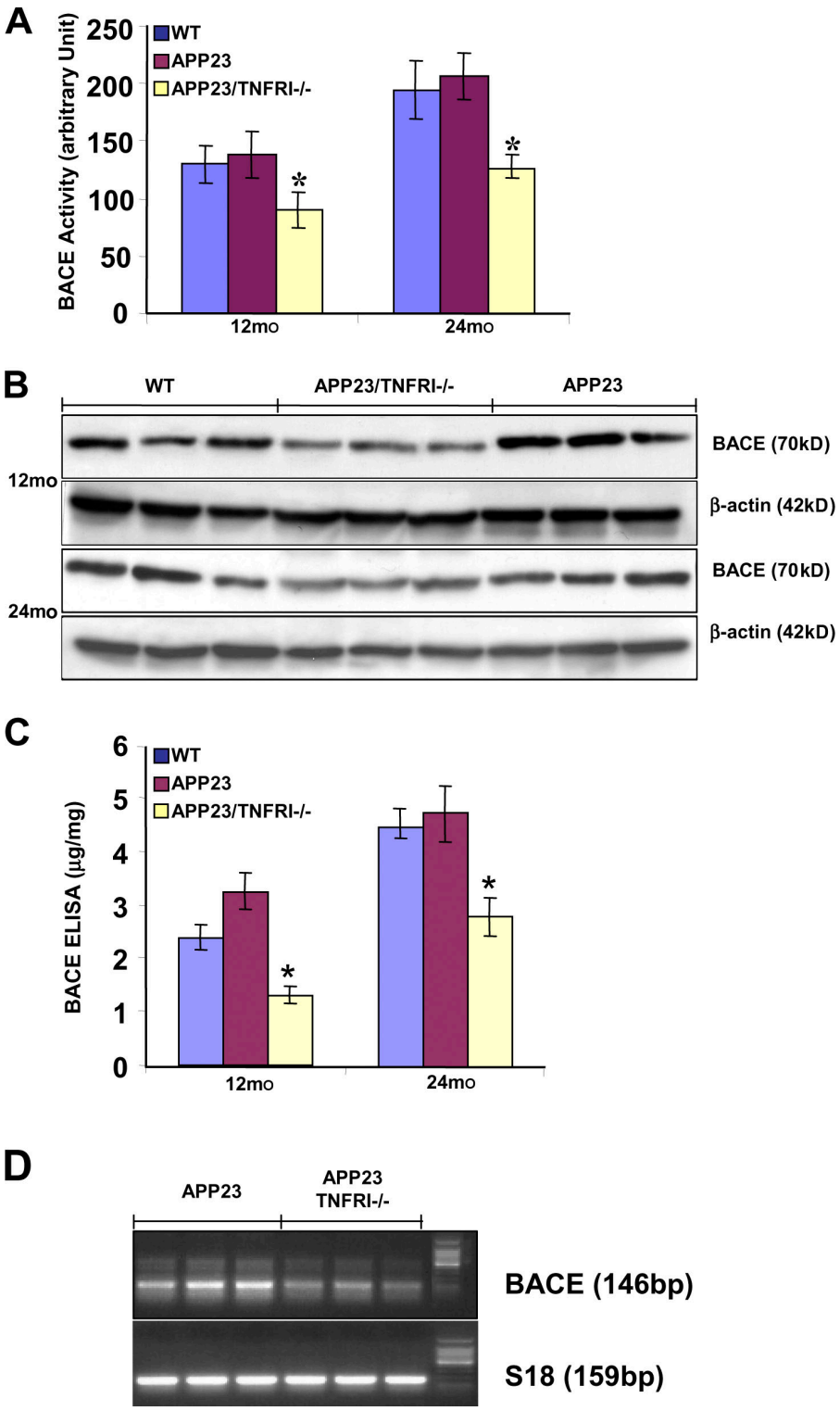

Figure 5. **Deletion of *TNFR1* reduced BACE1 protein levels and activity.** (A) BACE1 activity assay showed reduced BACE1 activity in APP23/*TNFR1*$^{-/-}$ mice at 12 and 24 mo, compared with APP23 mice. The activity was normalized to the input protein amount and indicated as an arbitrary unit (*, $P < 0.05$). (B) Western blot of BACE1 in wild-type, APP23/*TNFR1*$^{-/-}$, and APP23 mice. BACE1 expression levels were reduced in APP23/*TNFR1*$^{-/-}$ mice. (C) BACE1 ELISA showed that the BACE1 level was reduced in APP23/*TNFR1*$^{-/-}$ mice compared with APP23 and wild-type mice. BACE1 concentrations were calculated using a BACE1 standard curve. Concentrations are expressed as microgram per milligram of total protein (*, $P < 0.05$). (D) RT-PCR of BACE1 from the brains of APP23 and APP23/*TNFR1*$^{-/-}$ mice, mouse ribosomal subunit protein s18 was used as a loading control. BACE1 mRNA was decreased in APP23/*TNFR1*$^{-/-}$ mice. Error bars represent SD.

age-matched wild-type mice. In addition, within-group *t*-test analyses confirmed that APP23/*TNFR1*$^{-/-}$ mice ($t = 8.872$, $P < 0.001$) and wild-type mice ($t = 10.024$, $P < 0.001$) performed above chance values (50%), whereas APP23 mice did not ($t = 0.092$). This result suggests that deletion of *TNFR1* in APP23 mice not only improves learning and memory in the hole-board behavioral test but also enhances performance in objective recognition.

Discussion

TNFR is a family of TNF receptors, *TNFR1* and *TNFR2* (Tartaglia et al., 1993), both of which bind soluble Aβ40 (Li et al., 2004b). Overexpression of *TNFR1* promotes Aβ-induced neuronal death (Li et al., 2004b). It has been reported that a higher inflammatory response was observed in MCI and AD patients (Cagnin et al., 2001; Tarkowski et al., 2003 ;Galimberti et al., 2006),

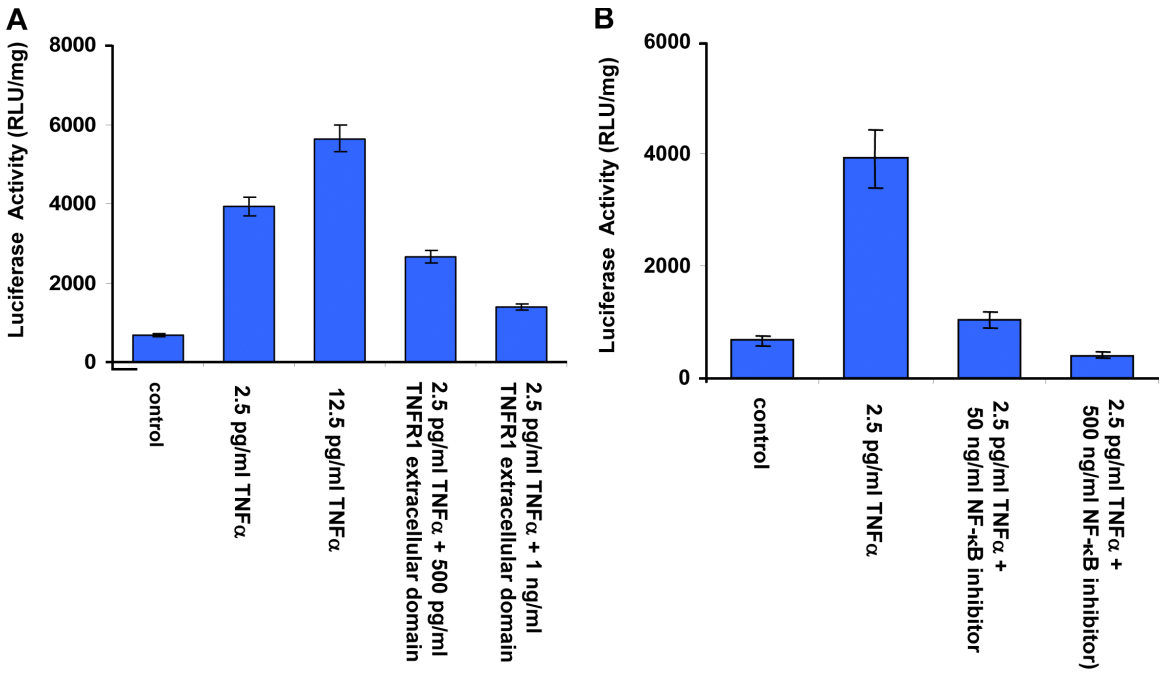

Figure 6. ***TNFR1* regulates BACE1 promoter activity through NF-κB.** (A) TNFα induces BACE1 promoter activity. (B) NF-κB inhibits TNFα-induced BACE1 promoter activity. Error bars represent SD.

and inflammatory cytokines and free radicals can up-regulate BACE1 expression (Tamagno et al., 2002; Hong et al., 2003; Pak et al., 2005; Tamagno et al., 2005; Sastre et al., 2006). TNFα is one of the up-regulated inflammation factors in APP transgenic mice (Patel et al., 2005). Here we found that *TNFR1* could directly regulate BACE1 transcription through NF-κB, which is one of the major mediators of TNFα-activated *TNFR1* signaling (Hsu et al., 1995; Yang et al., 2002). Recent findings showed multiple NF-κB binding sites located in the vicinity of BACE1 promoter (Sambamurti et al., 2004), suggesting that NF-κB may play an important role in regulating BACE1 transcription. This is confirmed by our results that the NF-κB inhibitor inhibits BACE1 promoter activity.

At 24 mo of age, we found significant neuronal loss in APP23 mice. However, Irizarry et al. (1997) did not observe neuronal loss in 16-mo-old APP transgenic mice (Tg2576) expressing the APPK670N/M671L mutation, the same mutation harbored by APP23 mice. This might be because the APP transgene is controlled by different promoters in APP23 and Tg2576 mice (Irizarry et al., 1997; Sturchler-Pierrat et al., 1997). *TNFR1* deficiency ameliorates neuron loss in APP23 mice, consistent with our previous findings that *TNFR1* overexpression increases the vulnerability of cultured hippocampal neurons to Aβ-induced death and promotes neuronal degeneration (Li et al., 2004b). We also noticed that TNFα plays different roles in neuronal death and survival via its distinct receptors, *TNFR1* and *TNFR2*. Neuron loss in APP23 mice caused by "endogenous" Aβ may be conducted through different signal transduction pathways. Moreover, Barger et al. (1995) showed that TNFα can protect neurons derived from fetal brains against Aβ toxicity. Our unpublished data show that *TNFR1* is expressed at a low level, whereas *TNFR2* is expressed at a high level in fetal neurons. This may explain why TNFα is trophic in fetal neurons. Interestingly, Bruce et al. (1996) discovered that neurons from mice with a deficiency of both *TNFR1* and *TNFR2* are more sensitive to excitotoxic injury. This result is interesting because the finding suggests that there is a balance between *TNFR1* and *TNFR2* expression levels in neurons, and *TNFR2* seems to be more critical and more sensitive to neurons.

Our behavioral analyses revealed that inactivation of *TNFR1* rescued hippocampal-dependent learning and memory deficits displayed by young APP23 mice (Van Dam et al., 2003). A previous study reported that disruption of the *BACE1* gene or PS1 in APP transgenic mice rescues memory deficits measured by social recognition and spatial alternation tasks (Saura et al., 2005). This is consistent with our findings in APP23/*TNFR1*$^{-/-}$ mice, presumably because *TNFR1* depletion decreases Aβ production and deposition, thereby reducing Aβ-related memory deficits. The relatively normal performance of hippocampal-dependent memory tasks by APP23/*TNFR1*$^{-/-}$ mice is age related. At 6 mo of age, APP23/*TNFR1*$^{-/-}$ mice already performed hippocampal-dependent memory tasks better than APP23 mice. Furthermore, *TNFR1* knockout mice exhibited normal synaptic transmission and plasticity in the Schaffer collateral pathway (unpublished data). Our results allow us to determine whether treating APP23 mice with anti-TNFR1 antibody or inhibitors of the *TNFR1* signal transduction pathway could reduce BACE1 and cerebral Aβ.

Materials and methods

Generation of APP transgenic AD mice with deletion of *TNFR1*

TNFR1 knockout mice (*TNFR1*$^{-/-}$) were constructed on a C57BL/6 background as previously described (Peschon et al., 1998). APP23 transgenic mice were provided by Novartis Institute for Biomedical Research; these

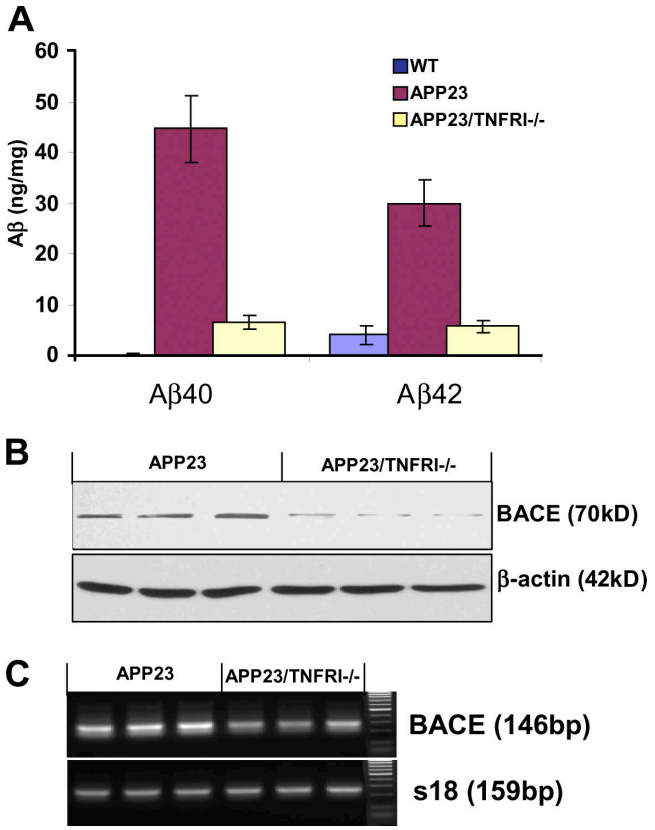

Figure 7. **Aβ and BACE1 levels are reduced in APP23/*TNFR1*$^{-/-}$ mice as early as 6 mo of age.** (A) Aβ40 and Aβ42 levels of APP23 and APP23/*TNFR1*$^{-/-}$ mice at 6 mo of age. (B) Western blots showed that BACE1 in APP23/*TNFR1*$^{-/-}$ mice is much lower than that in PP23 mice at 6 mo of age. (C) RT-PCR showed that BACE1 mRNA in APP23/*TNFR1*$^{-/-}$ mice is significantly lower compared with APP23 mice at 6 mo of age. Error bars represent SD.

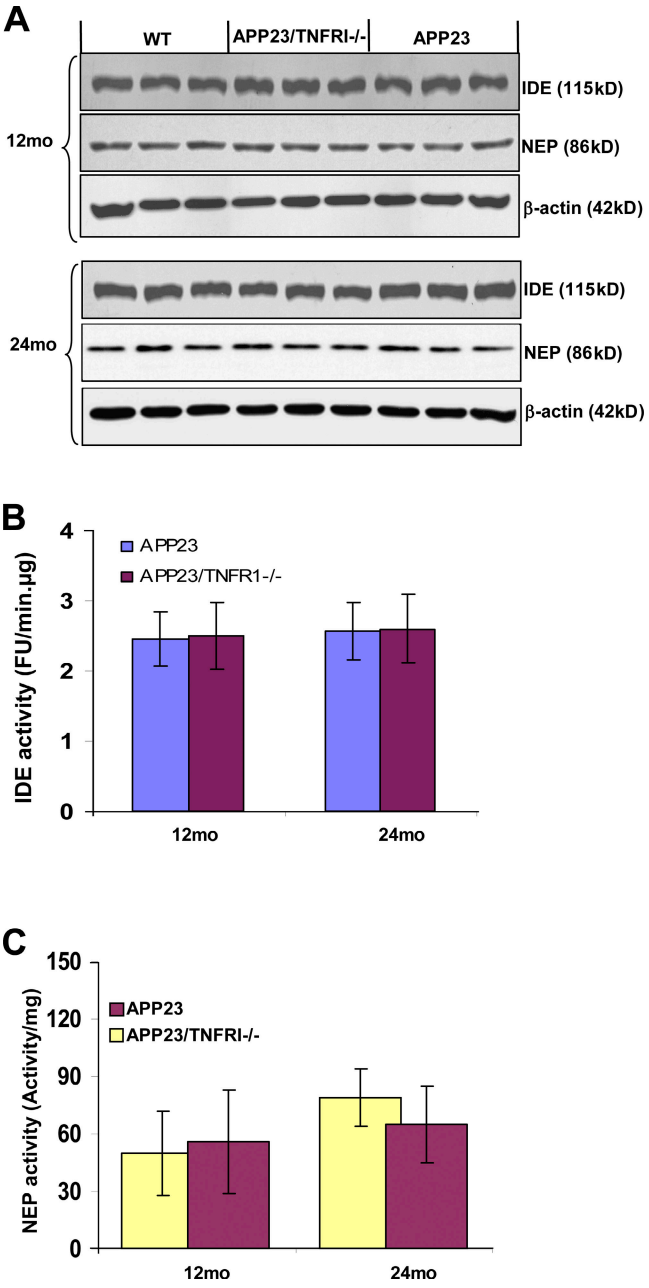

Figure 8. **Deletion of *TNFR1* has no effect on IDE or NEP.** (A) Western blots showing the density of IDE and NEP in brain lysates of wild-type, APP23/*TNFR1*$^{-/-}$,and APP23 mice at 12 and 24 mo of age. (B) No significant changes were observed in IDE activity between APP23 and APP23/*TNFR1*$^{-/-}$ mice. (C) No significant differences in NEP activity between APP23 and APP23/*TNFR1*$^{-/-}$ mice were found. Error bars represent SD.

mice express mutant human βAPP (Swedish double mutation, KM670/671NL) under the control of a brain- and neuron-specific murine Thy-1 promoter element. APP23 transgenic mice develop senile plaques in the cerebral cortex and hippocampus and show neuronal loss at 12–18 mo of age; this pathology is most evident in area CA1 of the hippocampus (Sommer and Staufenbiel, 1998). APP23 mice were also constructed on a C57BL/6 background.

APP23 and *TNFR1*$^{-/-}$ mice were crossed and their progeny were genotyped. An APP23/*TNFR1*$^{+/-}$ mouse was backcrossed with *TNFR1*$^{-/-}$ mice to produce APP23/*TNFR1*$^{-/-}$ mice. To maintain the heterozygous APP transgene in our mice, we crossed APP23 mice with wild-type C57BL/6 mice. For APP23/*TNFR1*$^{-/-}$ mice, we crossed APP23/*TNFR1*$^{-/-}$ with *TNFR1*$^{-/-}$ mice for three to five generations. Therefore, both APP23 and APP23/*TNFR1*$^{-/-}$ mice were *APP23*$^{+/-}$. We used APP23/*TNFR1*$^{-/-}$ mice of the F3–F5 generation in our experiments.

Mice homozygous for the *TNFR1* targeted mutation (formerly *TNFR1*, p55 deficient) show defects in resistance to intracellular pathogens and are resistant to the lethal effects of lipopolysaccharide administration in conjunction with D-galactosamine. Pulmonary inflammatory responses are diminished in p55-deficient mice. There are also defects in splenic architecture, formation of germinal centers, and liver regeneration. *TNFR1*- deficient mice display increased susceptibility to atherosclerosis when maintained on a high-fat diet (Peschon et al., 1998). No observations regarding any syndromes of the central nervous system have been made.

ELISA

APP23, APP23/*TNFR1*$^{-/-}$, and wild-type mice (n = 10 per group) were killed at 12 and 24 mo of age, and one hemisphere of the brain was homogenized in homogenization buffer (250 mM sucrose, 20 mM Tris-HCl, pH 7.4, 1 mM EDTA, and 1 mM EGTA). An aliquot of the homogenate was dissolved in formic acid and neutralized with a neutralization buffer (1 mM Tris and 0.5 M Na_2HPO_4). Protein concentration was measured by protein assay (Bio-Rad Laboratories). For total Aβ ELISA, the capture antibody was monoclonal anti-Aβ antibody 4G8 (Chemicon), and the detection antibody was biotinylated monoclonal antibody anti-Aβ 6E10 (AbD Serotec). Aβ40 and Aβ42 were measured with an Aβ40 and Aβ42 ELISA kit (Biosource International). The ELISA system has been extensively tested and no cross-reactivity between Aβ40 and Aβ42 was observed. Data are presented as means ± SD of four experiments.

BACE1 protein levels were measured by ELISA as described previously (Yang et al., 2003). The capture antibody was anti-BACE1 polyclonal antibody P1 (Yang et al., 2003) and the detection antibody was biotinylated anti-BACE1 polyclonal antibody P2 (Yang et al., 2003). TMB substrate was used to visualize the reaction product, which was

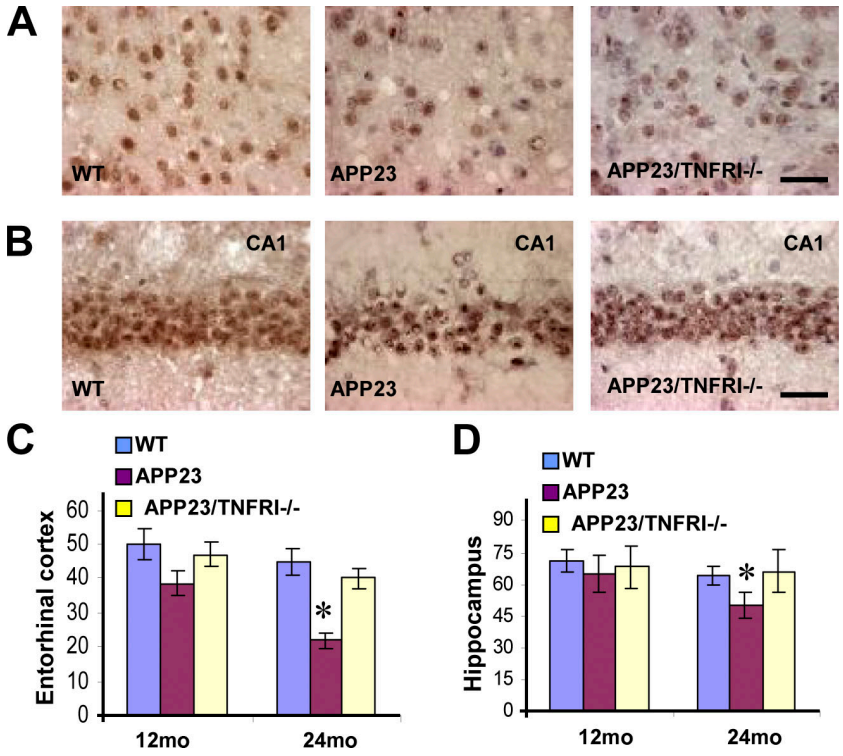

Figure 9. **Deletion of *TNFR1* in APP23 mice reduces neuron loss.** (A) Fewer NeuN-positive neurons were present in the entorhinal cortex of APP23 mice at the age of 24 mo. (B) NeuN immunostaining demonstrated little neuronal loss in the CA1 field in APP23/*TNFR1*$^{-/-}$ mice. (C) Statistical analyses show that APP23 mice had significantly fewer neurons in the entorhinal cortex at 24 mo of age (*, $P < 0.01$). (D) Statistical analyses show APP23 mice had significantly fewer neurons in the CA1 of the hippocampus at 24 mo of age (*, $P < 0.01$). Error bars represent SD. Bars, 10 μm.

read at OD_{450} with a microplate reader (Sigma-Aldrich). BACE1 protein (Amgen) was used as a standard. Data are presented as means ± SD of four experiments.

Western blot

Aliquots of brain homogenates from APP23, APP23/*TNFR1*$^{-/-}$, and wild-type mice were further lysed with 1× RIPA buffer, and 50–150 μg of total protein was subjected to SDS-PAGE (8–12% acrylamide). Separated proteins were then transferred onto polyvinylidene fluoride membranes. The blots were probed with the following antibodies: anti-BACE1 monoclonal antibody (R&D Systems), anti-Aβ (1–17) monoclonal antibody (clone 6E10, 1:2,000; Chemicon), anti-IDE polyclonal antibody (Oncogene Research Products), anti-NEP polyclonal antibody (Chemicon), and anti–β actin antibody (Sigma-Aldrich).

Western blotting for Aβ was performed as described previously (Wiltfang et al., 1997). To detect minute levels of Aβ, formic acid–dissolved brain tissue was immunoprecipitated with anti-Aβ polyclonal antibody (Zymed Laboratories) and subjected to SDS-PAGE using 10% acrylamide gels containing 8 M urea. Separated proteins were transferred onto polyvinylidene fluoride membranes. Aβ40 and Aβ42 were detected with monoclonal anti-Aβ antibody 6E10. Synthetic Aβ40 and Aβ42 (Biosource International) were used as standards.

BACE1, IDE, and NEP activity

An aliquot of brain homogenates from APP23, APP23/*TNFR1*$^{-/-}$, and wild-type mice was further lysed with a lysis buffer (10 mM Tris-HCl, pH 7.4, 150 mM NaCl, 1 mM EDTA, 1 mM EGTA, 1 mM Na_3VO_4, 10% glycerol, and 0.5% Triton X-100). BACE1 enzymatic activity assays were performed by using synthetic peptide substrates containing BACE1 cleavage site (MCA-Glu-Val-Lys-Met-Asp-Ala-Glu-Phe-[Lys-DNP]-OH; Biosource International). BACE substrate was dissolved in DMSO and mixed with a 50-mM Hac and 100-mM NaCl, pH 4.1, reaction buffer. An equal amount of protein was mixed with 100 μl of substrate, and fluorescence intensity was measured with a microplate reader (BioTek) at an excitation wavelength of 320 nm and an emission wavelength of 390 nm.

IDE enzyme activity was measured as described previously (Song et al., 2003). In brief, brains were homogenized in 50 mM potassium phosphate buffer, pH 7.3, containing 200 μm PMSF and a proteinase inhibitor mix (Sigma-Aldrich). Samples were centrifuged and the supernatant fraction was used for IDE activity measurement. The hydrolysis of fluorogenic substrate peptides (2 μm Abz-GGFLRKHGQED-Dnp as substrate in 20 mM potassium phosphate buffer, pH 7.3) was measured by following an increase in fluorescence (excitation at 318 nm and emission at 419 nm) that occurred upon peptide bond cleavage. The max velocity of IDE activity was calculated by the first 20 min and indicated as fluorescence unit/min microgram protein.

For the in vitro NEP activity assay, mouse brains were homogenized in 100 mM MES buffer (pH 6.5) with proteinase inhibitors (Sigma-Aldrich). Homogenate was centrifuged at 20,000 *g* for 45 min to separate the membrane fraction and the supernatant was removed. The membrane pellet was resuspended in MES buffer and directly used in NEP activity assay as previously described (Li and Hersh, 1995).

RT-PCR

To compare BACE1 expression levels, we used the following primers for RT-PCR: mouse BACE1 forward primer, 5′-AGACGCTACACATCCTGGTG-3′, and backward primer, 5′-CCTGGGTGTAGGGCACATAC-3′. The amplified BACE1 fragment was 146 bp. Mouse s18 was used as a loading control: forward primer, 5′-CAGAAGGACGTGAAGGATGG-3′, and backward primer, 5′-CAGTGGTCTTGGTGTGCTGA-3′. The amplified mouse s18 fragment was 159 bp. Total RNA was extracted from the brains of 12-mo-old APP23 and APP23/*TNFR1*$^{-/-}$ mice ($n = 5$) using an RNA mini column kit (Invitrogen). RT-PCR was performed using a One- Step RT-PCR kit (Invitrogen) and the following PCR cycles: 50°C for 30 min, 94°C for 2 min, followed by 25 cycles at 94°C for 15 s, 49°C for 30 s, and 68°C for 1 min.

Cell transfection and luciferase assay

We transfected 293 cells with pB1P-A vector containing a *BACE1* promoter (−1941 to +292) upstream from a luciferase reporter gene (Christensen et al., 2004) using lipofectamine (Invitrogen). After transfection, cells were treated with different concentrations of TNFα (R&D Systems), extracellular domain of TNFR1 (R&D Systems), or NF-κB inhibitor 6-amino-4(4-phenoxyphenylethylamino) quinazoline (Calbiochem; Tobe et al., 2003). Cells were collected 12 h after treatment, and a luciferase assay (Promega) was performed, according to the manufacturer's instructions. Luminescence intensity was measured with a microplate reader, normalized according to protein amount, and plotted as relative luminescence units per milligram of protein.

Immunohistochemistry and immunofluorescence

Immunohistochemistry was performed as previously described (Matsuoka et al., 2001). In brief, paraformaldehyde-fixed brains were quickly frozen, and then sectioned at 30 μm. Sections were incubated with either anti-Aβ (6E10 clone or 4G8 clone, 1:1,000; Chemicon), anti-NeuN (MAB377,

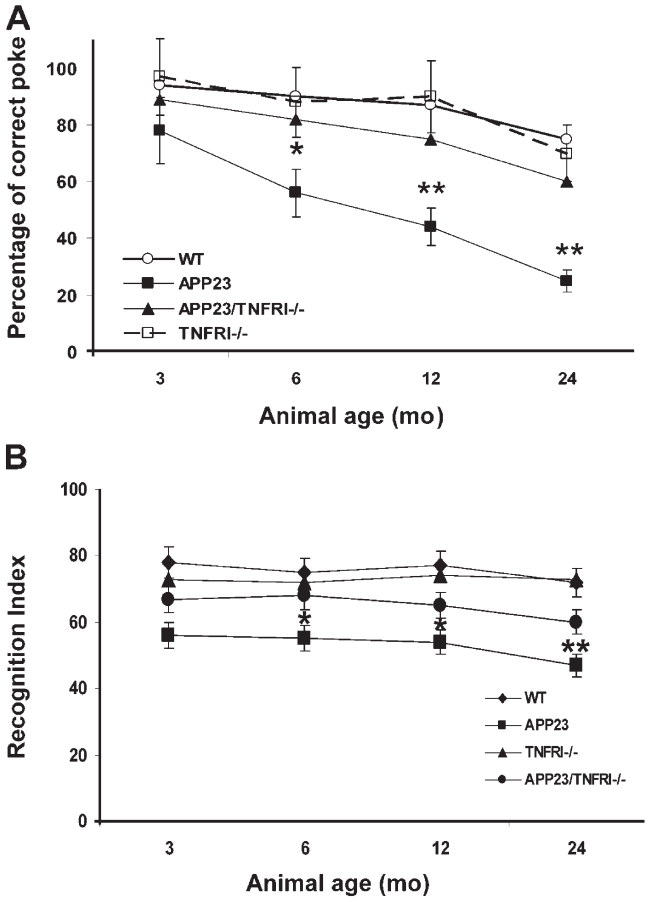

Figure 10. **Deletion of *TNFR1* improves learning and memory.** (A) The percentage correct of finding a cheese reward hidden in one hole of the hole-board task (Brosnan-Watters and Wozniak, 1997). Data were calculated as percentages (mean ± SEM; *, $P < 0.05$; **, $P < 0.001$). (B) Object recognition memory performance was superior in APP23/*TNFR1*$^{-/-}$ mice. The values represent the recognition index (mean ± SEM). The same genotype and age groups were tested as the hole-board task.

1:400; Chemicon), anti-CD11b (MCA711, 1:500; AbD Serotec) and CD45 (MCA1388, 1:500; AbD Serotec), anti-α-smooth muscle actin (α-SM actin, A2547, 1:400; Sigma-Aldrich), or anti-vWF (AB7536, 1:200; Chemicon). Secondary antibodies were applied with horse anti–mouse (for 6E10, NeuN detection, 1:1,000) and goat anti–rat (for CD45 or CD11b, 1:1,000) followed by a DAB substrate (Vector Laboratories). For immunofluorescence, fluorescent-labeling 488 (green) or 594 (red) secondary antibodies against rabbit IgG or mouse IgG were used (1:1,000; Invitrogen). A microscope (DMLS; Leica) with a 10× N PLAN and 20× and 40× PL FLUOTAR was used. Digital images were captured and processed by digital camera (Optronics) and MagnaFire software (version 2.1C; Optronics).

Quantitation of immunoreactive structures

30-μm serial sagittal sections through the entire rostrocaudal extent of the hippocampus were cut on a cryostat. Every 10th section was immunostained with anti-NeuN antibody. On all sections containing the hippocampus, we delineated the pyramidal cell layer CA1. The total number of neurons were obtained using unbiased stereology (Casas et al., 2004; Schmitz et al., 2004) and a microscope equipped with a digital camera (DEI-470; Optronics). For each section, we delineated a 400-μm^2 area in CA1 and in the entorhinal cortex and counted all NeuN-immunoreactive cells within that 400-μm^2 box. The mean sum of neurons was counted per animal ($n = 10$). We used the same method to count Aβ-immunoreactive plaques (stained with 6E10) in the hippocampus and entorhinal cortex in a double blind test. We also measured the diameter of each counted plaque. Differences between groups were tested with Image-pro Plus Analysis (Media Cybernetics).

Hole-board memory task

As previously reported (Dodart et al., 2002), this task measured a mouse's ability to remember which one out of four equidistant holes was baited with food. Two photobeam apparatuses were used with a hole board for assessing directed exploration in mice for behavioral tests. A tested mouse ($n = 10$ for each group) was placed in the center of the hole-board and the number of nose pokes was automatically registered for 5 min. After 20 min, each animal was placed in a corner of the hole board and allowed to freely explore the apparatus for 5 min. The number of head dips, time spent head-dipping, and the number of rearings were recorded. A comprehensive cognitive performance was determined by calculating the mean number of correct pokes per trial that mouse made each day. Cognition was expressed as the percentage of correct pokes. The measurements in the hole-board test were analyzed by unpaired *t* test. In all cases the significance level was considered to be $P < 0.05$, and the very significant level was considered to be $P < 0.01$.

Object recognition task

The day before training, an individual mouse ($n = 10$ for each group) was placed into a training apparatus (a box the same size as described for the hole-board test) and allowed to habituate to the environment for 15 min. Training was initiated 24 h after habituation. A mouse was placed back into the training box containing two identical objects A and B (die or marble) and allowed to explore these objects. Among experiments, training times varied from 3.5 to 20 min. For each experiment, the same set of animals was used repeatedly with different sets of objects for each repetition. Five repetitions were performed on each set of mice. Each mouse was trained and tested no more than once per week, with a 1-wk interval between testing. Moreover, each experimental condition was replicated independently four times. In each experiment, the experimenter was blinded to the subjects during training and testing. To test memory retention, mice were observed for 10 min, 6 h, and 24 h after training. Mice were presented with two objects, one that was used during training, and thus was "familiar," and one that was novel. The test objects were divided into 10 sets of "training" plus "testing" objects, and a new set of objects was used for each training session. A recognition index was calculated for each mouse, expressed as the ratio (100TB)×(TA + TB), where TA and TB are the time spent during the second trial on subject A and subject B, respectively. To ensure that the discrimination targets did not differ in odor, the apparatus and the objects were thoroughly cleaned with 90% ethanol, dried, and ventilated for a few minutes after each experiment.

Statistical analyses

In general, analysis of variance models (ANOVA) were used to analyze behavioral data. Typically, the statistical models included two between-subjects variables, the genotype of mice (APP23 vs. APP23/*TNFR1*$^{-/-}$) and age, and one within-subjects variable, such as blocks of trials. When ANOVAs with repeated measures were conducted, the Huynh-Feldt adjustment of α levels was used for all within-subjects effects containing more than two levels to protect against violations of the sphericity/compound symmetry assumptions underlying this ANOVA model.

This work was, in part, supported by the Alzheimer's Association, the Arizona Biomedical Research Consortium (ADRC0020), and the National Institute on Aging (AG025888).

Submitted: 8 May 2007
Accepted: 25 July 2007

References

Ashkenazi, A., and V.M. Dixit. 1998. Death receptors: signaling and modulation. *Science*. 281:1305–1308.

Atwood, C.S., G. Perry, and M.A. Smith. 2003. Cerebral hemorrhage and amyloid-beta. *Science*. 299:1014.

Barger, S.W., D. Horster, K. Furukawa, Y. Goodman, J. Krieglstein, and M.P. Mattson. 1995. Tumor necrosis factors alpha and beta protect neurons against amyloid beta-peptide toxicity: evidence for involvement of a kappa B-binding factor and attenuation of peroxide and Ca2+ accumulation. *Proc. Natl. Acad. Sci. USA*. 92:9328–9332.

Boldin, M.P., I.L. Mett, E.E. Varfolomeev, I. Chumakov, Y. Shemer-Avni, J.H. Camonis, and D. Wallach. 1995. Self-association of the "death domains" of the p55 tumor necrosis factor (TNF) receptor and Fas/APO1 prompts signaling for TNF and Fas/APO1 effects. *J. Biol. Chem.* 270:387–391.

Bourtchouladze, R., R. Lidge, R. Catapano, J. Stanley, S. Gossweiler, D. Romashko, R. Scott, and T. Tully. 2003. A mouse model of Rubinstein-Taybi syndrome: defective long-term memory is ameliorated by inhibitors of phosphodiesterase 4. *Proc. Natl. Acad. Sci. USA*. 100:10518–10522.

Brosnan-Watters, G., and D.F. Wozniak. 1997. A rotating holeboard procedure for testing drug effects on spatial learning and memory in mice. *Brain Res. Brain Res. Protoc.* 1:331–338.

Bruce, A.J., W. Boling, M.S. Kindy, J. Peschon, P.J. Kraemer, M.K. Carpenter, F.W. Holtsberg, and M.P. Mattson. 1996. Altered neuronal and microglial responses to excitotoxic and ischemic brain injury in mice lacking TNF receptors. *Nat. Med.* 2:788–794.

Cagnin, A., D.J. Brooks, A.M. Kennedy, R.N. Gunn, R. Myers, F.E. Turkheimer, T. Jones, and R.B. Banati. 2001. In-vivo measurement of activated microglia in dementia. *Lancet*. 358:461–467.

Calhoun, M.E., K.H. Wiederhold, D. Abramowski, A.L. Phinney, A. Probst, C. Sturchler-Pierrat, M. Staufenbiel, B. Sommer, and M. Jucker. 1998. Neuron loss in APP transgenic mice. *Nature*. 395:755–756.

Calhoun, M.E., P. Burgermeister, A.L. Phinney, M. Stalder, M. Tolnay, K.H. Wiederhold, D. Abramowski, C. Sturchler-Pierrat, B. Sommer, M. Staufenbiel, and M. Jucker. 1999. Neuronal overexpression of mutant amyloid precursor protein results in prominent deposition of cerebrovascular amyloid. *Proc. Natl. Acad. Sci. USA*. 96:14088–14093.

Casas, C., N. Sergeant, J.M. Itier, V. Blanchard, O. Wirths, N. van der Kolk, V. Vingtdeux, E. van de Steeg, G. Ret, T. Canton, et al. 2004. Massive CA1/2 neuronal loss with intraneuronal and N-terminal truncated Abeta42 accumulation in a novel Alzheimer transgenic model. *Am. J. Pathol.* 165:1289–1300.

Christensen, M.A., W. Zhou, H. Qing, A. Lehman, S. Philipsen, and W. Song. 2004. Transcriptional regulation of BACE1, the beta-amyloid precursor protein beta-secretase, by Sp1. *Mol. Cell. Biol.* 24:865–874.

Cohen, D.L., P. Hedera, D.R. Premkumar, R.P. Friedland, and R.N. Kalaria. 1997. Amyloid-beta protein angiopathies masquerading as Alzheimer's disease? *Ann. NY Acad. Sci.* 826:390–395.

Dodart, J.C., K.R. Bales, K.S. Gannon, S.J. Greene, R.B. DeMattos, C. Mathis, C.A. DeLong, S. Wu, X. Wu, D.M. Holtzman, and S.M. Paul. 2002. Immunization reverses memory deficits without reducing brain Abeta burden in Alzheimer's disease model. *Nat. Neurosci.* 5:452–457.

Farris, W., S. Mansourian, Y. Chang, L. Lindsley, E.A. Eckman, M.P. Frosch, C.B. Eckman, R.E. Tanzi, D.J. Selkoe, and S. Guenette. 2003. Insulin-degrading enzyme regulates the levels of insulin, amyloid beta-protein, and the beta-amyloid precursor protein intracellular domain in vivo. *Proc. Natl. Acad. Sci. USA*. 100:4162–4167.

Frid, P., S.V. Anisimov, and N. Popovic. 2007. Congo red and protein aggregation in neurodegenerative diseases. *Brain Res. Rev.* 53:135–160.

Galimberti, D., N. Schoonenboom, P. Scheltens, C. Fenoglio, F. Bouwman, E. Venturelli, I. Guidi, M.A. Blankenstein, N. Bresolin, and E. Scarpini. 2006. Intrathecal chemokine synthesis in mild cognitive impairment and Alzheimer disease. *Arch. Neurol.* 63:538–543.

Garcia, J. 1987. Sharing research results with patients: the views of care-givers involved in a randomized controlled trial. *J. Reprod. Infant Psychol.* 5:9–13.

Hebert, L.E., P.A. Scherr, J.L. Bienias, D.A. Bennett, and D.A. Evans. 2003. Alzheimer disease in the US population: prevalence estimates using the 2000 census. *Arch. Neurol.* 60:1119–1122.

Hong, H.S., E.M. Hwang, H.J. Sim, H.J. Cho, J.H. Boo, S.S. Oh, S.U. Kim, and I. Mook-Jung. 2003. Interferon gamma stimulates beta-secretase expression and sAPPbeta production in astrocytes. *Biochem. Biophys. Res. Commun.* 307:922–927.

Hsiao, K.K., D.R. Borchelt, K. Olson, R. Johannsdottir, C. Kitt, W. Yunis, S. Xu, C. Eckman, S. Younkin, D. Price, et al. 1995. Age-related CNS disorder and early death in transgenic FVB/N mice overexpressing Alzheimer amyloid precursor proteins. *Neuron*. 15:1203–1218.

Hsu, H., J. Xiong, and D.V. Goeddel. 1995. The TNF receptor 1-associated protein TRADD signals cell death and NF-kappa B activation. *Cell*. 81:495–504.

Irizarry, M.C., M. McNamara, K. Fedorchak, K. Hsiao, and B.T. Hyman. 1997. APPSw transgenic mice develop age-related A beta deposits and neuropil abnormalities, but no neuronal loss in CA1. *J. Neuropathol. Exp. Neurol.* 56:965–973.

Itoh, Y., M. Yamada, M. Hayakawa, E. Otomo, and T. Miyatake. 1993. Cerebral amyloid angiopathy: a significant cause of cerebellar as well as lobar cerebral hemorrhage in the elderly. *J. Neurol. Sci.* 116:135–141.

Li, C., and L.B. Hersh. 1995. Neprilysin: assay methods, purification, and characterization. *Methods Enzymol.* 248:253–263.

Li, R., K. Lindholm, L.B. Yang, X. Yue, M. Citron, R. Yan, T. Beach, L. Sue, M. Sabbagh, H. Cai, et al. 2004a. Amyloid beta peptide load is correlated with increased beta-secretase activity in sporadic Alzheimer's disease patients. *Proc. Natl. Acad. Sci. USA*. 101:3632–3637.

Li, R., L. Yang, K. Lindholm, Y. Konishi, X. Yue, H. Hampel, D. Zhang, and Y. Shen. 2004b. Tumor necrosis factor death receptor signaling cascade is required for amyloid-beta protein-induced neuron death. *J. Neurosci.* 24:1760–1771.

Matsuoka, Y., M. Picciano, B. Malester, J. LaFrancois, C. Zehr, J.M. Daeschner, J.A. Olschowka, M.I. Fonseca, M.K. O'Banion, A.J. Tenner, et al. 2001. Inflammatory responses to amyloidosis in a transgenic mouse model of Alzheimer's disease. *Am. J. Pathol.* 158:1345–1354.

Pak, T., P. Cadet, K.J. Mantione, and G.B. Stefano. 2005. Morphine via nitric oxide modulates beta-amyloid metabolism: a novel protective mechanism for Alzheimer's disease. *Med. Sci. Monit.* 11:BR357–BR366.

Patel, N.S., D. Paris, V. Mathura, A.N. Quadros, F.C. Crawford, and M.J. Mullan. 2005. Inflammatory cytokine levels correlate with amyloid load in transgenic mouse models of Alzheimer's disease. *J. Neuroinflammation*. 2:9.

Peschon, J.J., D.S. Torrance, K.L. Stocking, M.B. Glaccum, C. Otten, C.R. Willis, K. Charrier, P.J. Morrissey, C.B. Ware, and K.M. Mohler. 1998. TNF receptor-deficient mice reveal divergent roles for p55 and p75 in several models of inflammation. *J. Immunol.* 160:943–952.

Pittenger, C., Y.Y. Huang, R.F. Paletzki, R. Bourtchouladze, H. Scanlin, S. Vronskaya, and E.R. Kandel. 2002. Reversible inhibition of CREB/ATF transcription factors in region CA1 of the dorsal hippocampus disrupts hippocampus-dependent spatial memory. *Neuron*. 34:447–462.

Sambamurti, K., R. Kinsey, B. Maloney, Y.W. Ge, and D.K. Lahiri. 2004. Gene structure and organization of the human beta-secretase (BACE) promoter. *FASEB J.* 18:1034–1036.

Sastre, M., I. Dewachter, S. Rossner, N. Bogdanovic, E. Rosen, P. Borghgraef, B.O. Evert, L. Dumitrescu-Ozimek, D.R. Thal, G. Landreth, et al. 2006. Nonsteroidal anti-inflammatory drugs repress beta-secretase gene promoter activity by the activation of PPARgamma. *Proc. Natl. Acad. Sci. USA*. 103:443–448.

Saura, C.A., G. Chen, S. Malkani, S.Y. Choi, R.H. Takahashi, D. Zhang, G.K. Gouras, A. Kirkwood, R.G. Morris, and J. Shen. 2005. Conditional inactivation of presenilin 1 prevents amyloid accumulation and temporarily rescues contextual and spatial working memory impairments in amyloid precursor protein transgenic mice. *J. Neurosci.* 25:6755–6764.

Schmitz, C., B.P. Rutten, A. Pielen, S. Schafer, O. Wirths, G. Tremp, C. Czech, V. Blanchard, G. Multhaup, P. Rezaie, et al. 2004. Hippocampal neuron loss exceeds amyloid plaque load in a transgenic mouse model of Alzheimer's disease. *Am. J. Pathol.* 164:1495–1502.

Selkoe, D.J. 2003. Aging, amyloid, and Alzheimer's disease: a perspective in honor of Carl Cotman. *Neurochem. Res.* 28:1705–1713.

Shyu, W.C., S.Z. Lin, M.F. Chiang, C.Y. Su, and H. Li. 2006. Intracerebral peripheral blood stem cell (CD34+) implantation induces neuroplasticity by enhancing beta1 integrin-mediated angiogenesis in chronic stroke rats. *J. Neurosci.* 26:3444–3453.

Simard, A.R., D. Soulet, G. Gowing, J.P. Julien, and S. Rivest. 2006. Bone marrow-derived microglia play a critical role in restricting senile plaque formation in Alzheimer's disease. *Neuron*. 49:489–502.

Skalli, O., P. Ropraz, A. Trzeciak, G. Benzonana, D. Gillessen, and G. Gabbiani. 1986. A monoclonal antibody against α-smooth muscle actin: a new probe for smooth muscle differentiation. *J. Cell Biol.* 103:2787–2796.

Sommer, B., and M. Staufenbiel. 1998. A beta peptide deposition in the brains of transgenic mice: evidence for a key event in Alzheimer's disease pathogenesis. *Mol. Psychiatry*. 3:284–286, 282–283.

Song, E.S., M.A. Juliano, L. Juliano, and L.B. Hersh. 2003. Substrate activation of insulin-degrading enzyme (insulysin). A potential target for drug development. *J. Biol. Chem.* 278:49789–49794.

Sturchler-Pierrat, C., D. Abramowski, M. Duke, K.H. Wiederhold, C. Mistl, S. Rothacher, B. Ledermann, K. Burki, P. Frey, P.A. Paganetti, et al. 1997. Two amyloid precursor protein transgenic mouse models with Alzheimer disease-like pathology. *Proc. Natl. Acad. Sci. USA*. 94:13287–13292.

Tamagno, E., P. Bardini, A. Obbili, A. Vitali, R. Borghi, D. Zaccheo, M.A. Pronzato, O. Danni, M.A. Smith, G. Perry, and M. Tabaton. 2002. Oxidative stress increases expression and activity of BACE in NT2 neurons. *Neurobiol. Dis.* 10:279–288.

Tamagno, E., M. Parola, P. Bardini, A. Piccini, R. Borghi, M. Guglielmotto, G. Santoro, A. Davit, O. Danni, M.A. Smith, et al. 2005. Beta-site APP cleaving enzyme up-regulation induced by 4-hydroxynonenal is mediated by stress-activated protein kinases pathways. *J. Neurochem.* 92:628–636.

Tanzi, R.E., and L. Bertram. 2005. Twenty years of the Alzheimer's disease amyloid hypothesis: a genetic perspective. *Cell*. 120:545–555.

Tarkowski, E., N. Andreasen, A. Tarkowski, and K. Blennow. 2003. Intrathecal inflammation precedes development of Alzheimer's disease. *J. Neurol. Neurosurg. Psychiatry*. 74:1200–1205.

Tartaglia, L.A., M. Rothe, Y.F. Hu, and D.V. Goeddel. 1993. Tumor necrosis factor's cytotoxic activity is signaled by the p55 TNF receptor. *Cell*. 73:213–216.

Terry, R.D., L.A. Hansen, R. DeTeresa, P. Davies, H. Tobias, and R. Katzman. 1987. Senile dementia of the Alzheimer type without neocortical neurofibrillary tangles. *J. Neuropathol. Exp. Neurol.* 46:262–268.

Thal, D.R., E. Ghebremedhin, M. Orantes, and O.D. Wiestler. 2003. Vascular pathology in Alzheimer disease: correlation of cerebral amyloid angiopathy and arteriosclerosis/lipohyalinosis with cognitive decline. *J. Neuropathol. Exp. Neurol.* 62:1287–1301.

Thifault, S., R. Lalonde, N. Sanon, and P. Hamet. 2002. Comparisons between C57BL/6J and A/J mice in motor activity and coordination, hole-poking, and spatial learning. *Brain Res. Bull.* 58:213–218.

Tian, J., J. Shi, K. Bailey, and D.M. Mann. 2003. Negative association between amyloid plaques and cerebral amyloid angiopathy in Alzheimer's disease. *Neurosci. Lett.* 352:137–140.

Tiraboschi, P., M.N. Sabbagh, L.A. Hansen, D.P. Salmon, A. Merdes, A. Gamst, E. Masliah, M. Alford, L.J. Thal, and J. Corey-Bloom. 2004. Alzheimer disease without neocortical neurofibrillary tangles: "a second look." *Neurology*. 62:1141–1147.

Tobe, M., Y. Isobe, H. Tomizawa, T. Nagasaki, H. Takahashi, T. Fukazawa, and H. Hayashi. 2003. Discovery of quinazolines as a novel structural class of potent inhibitors of NF-kappa B activation. *Bioorg. Med. Chem.* 11:383–391.

Van Dam, D., R. D'Hooge, M. Staufenbiel, C. Van Ginneken, F. Van Meir, and P.P. De Deyn. 2003. Age-dependent cognitive decline in the APP23 model precedes amyloid deposition. *Eur. J. Neurosci.* 17:388–396.

Van Dooren, T., D. Muyllaert, P. Borghgraef, A. Cresens, H. Devijver, I. Van der Auwera, S. Wera, I. Dewachter, and F. Van Leuven. 2006. Neuronal or glial expression of human apolipoprotein e4 affects parenchymal and vascular amyloid pathology differentially in different brain regions of double- and triple-transgenic mice. *Am. J. Pathol.* 168:245–260.

Vassar, R., B.D. Bennett, S. Babu-Khan, S. Kahn, E.A. Mendiaz, P. Denis, D.B. Teplow, S. Ross, P. Amarante, R. Loeloff, et al. 1999. Beta-secretase cleavage of Alzheimer's amyloid precursor protein by the transmembrane aspartic protease BACE. *Science*. 286:735–741.

Vinters, H.V. 1987. Cerebral amyloid angiopathy. A critical review. *Stroke*. 18:311–324.

Wang, H., G.D. Ferguson, V.V. Pineda, P.E. Cundiff, and D.R. Storm. 2004. Overexpression of type-1 adenylyl cyclase in mouse forebrain enhances recognition memory and LTP. *Nat. Neurosci.* 7:635–642.

Weiner, H.L., and D.J. Selkoe. 2002. Inflammation and therapeutic vaccination in CNS diseases. *Nature*. 420:879–884.

Wilcock, D.M., G. DiCarlo, D. Henderson, J. Jackson, K. Clarke, K.E. Ugen, M.N. Gordon, and D. Morgan. 2003. Intracranially administered anti-Abeta antibodies reduce beta-amyloid deposition by mechanisms both independent of and associated with microglial activation. *J. Neurosci.* 23:3745–3751.

Wilcock, D.M., A. Rojiani, A. Rosenthal, G. Levkowitz, S. Subbarao, J. Alamed, D. Wilson, N. Wilson, M.J. Freeman, M.N. Gordon, and D. Morgan. 2004. Passive amyloid immunotherapy clears amyloid and transiently activates microglia in a transgenic mouse model of amyloid deposition. *J. Neurosci.* 24:6144–6151.

Wiltfang, J., A. Smirnov, B. Schnierstein, G. Kelemen, U. Matthies, H.W. Klafki, M. Staufenbiel, G. Huther, E. Ruther, and J. Kornhuber. 1997. Improved electrophoretic separation and immunoblotting of beta-amyloid (A beta) peptides 1-40, 1-42, and 1-43. *Electrophoresis*. 18:527–532.

Winkler, D.T., L. Bondolfi, M.C. Herzig, L. Jann, M.E. Calhoun, K.H. Wiederhold, M. Tolnay, M. Staufenbiel, and M. Jucker. 2001. Spontaneous hemorrhagic stroke in a mouse model of cerebral amyloid angiopathy. *J. Neurosci.* 21:1619–1627.

Yan, Q., J. Zhang, H. Liu, S. Babu-Khan, R. Vassar, A.L. Biere, M. Citron, and G. Landreth. 2003. Anti-inflammatory drug therapy alters beta-amyloid processing and deposition in an animal model of Alzheimer's disease. *J. Neurosci.* 23:7504–7509.

Yang, L., K. Lindholm, Y. Konishi, R. Li, and Y. Shen. 2002. Target depletion of distinct tumor necrosis factor receptor subtypes reveals hippocampal neuron death and survival through different signal transduction pathways. *J. Neurosci.* 22:3025–3032.

Yang, L.B., K. Lindholm, R. Yan, M. Citron, W. Xia, X.L. Yang, T. Beach, L. Sue, P. Wong, D. Price, et al. 2003. Elevated beta-secretase expression and enzymatic activity detected in sporadic Alzheimer disease. *Nat. Med.* 9:3–4.

Zhou, J., M.I. Fonseca, R. Kayed, I. Hernandez, S.D. Webster, O. Yazan, D.H. Cribbs, C.G. Glabe, and A.J. Tenner. 2005. Novel Abeta peptide immunogens modulate plaque pathology and inflammation in a murine model of Alzheimer's disease. *J. Neuroinflammation*. 2:28.